PHYSICAL REVIEW B VOLUME 22, NUMBER 12 15 DECEMBER 1980

Resonance Raman scattering in InAs near the E_1 edge

R. Carles, N. Saint-Cricq, J. B. Renucci, A. Zwick, and M. A. Renucci

Laboratoire de Physique des Solides, Associé au Centre Nationale de la Recherche Scientifique, Université Paul Sabatier–118, Route de Narbonne, 31062 Toulouse Cédex, France

(Received 24 July 1980)

The resonance of several first-order [allowed TO(Γ), forbidden LO(Γ)] and second-order [2TA($\Delta \rightarrow K$),2TO(Δ,Σ,Λ),2LO(Γ)] structures of the Raman spectrum of InAs is investigated around the energy of the E_1 critical point. The deformation-potential coupling mechanism explains well the resonances of the 2TA($\Delta \rightarrow K$) and 2TO(Δ,Σ,Λ) whereas those of the 1LO(Γ) and 2LO(Γ) are accounted for by the Fröhlich interaction. Several electron–two-phonon deformation potentials are estimated. The sharp resonances of the 1LO(Γ) and 2LO(Γ) are followed over a wide range of temperatures (10–300 K). The results show clearly that the "Raman gap" differs from the optical one. It depends upon the phonons involved in contrast to its temperature dependence. This variation $(-5.0\pm0.4)\times10^{-4}$ eV K^{-1} agrees with that of the optical gap.

I. INTRODUCTION

Resonant Raman scattering has been studied in the vicinity of the E_0, $E_0+\Delta_0$ and E_1, $E_1+\Delta_1$ edges for a number of diamond and zinc-blende-type semiconductors.[1] In polar semiconductors two types of mechanisms are invoked to interpret the experimental results: the deformation-potential coupling and the Fröhlich coupling.[2] The allowed TO scattering includes both two-band and three-band terms. For the allowed LO scattering one has to add the contribution due to the interband term of the Fröhlich coupling.[3] Forbidden LO scattering, which appears near resonance, is explained by the intraband term of the Fröhlich interaction and is q dependent.

In InAs resonance measurements have been confined to first-order scattering.[4-8] Allowed TO(Γ) and LO(Γ) show the same resonance behavior.[4,5] The LO cross section is nevertheless stronger than the TO one[4,5] as expected from the additional contribution due to the intraband Fröhlich coupling. In forbidden configuration no resonance was detected for the weak TO(Γ) peak[4] whereas the forbidden LO(Γ) resonance was found much stronger than its allowed counterpart.[4,5] The second-order Raman spectra of InAs have been recently analyzed by Carles *et al.*[9] Figure 1 displays the Γ_1 and Γ_{15} components of the Raman spectra recorded at 100 K with an incident laser wavelength of 4880 Å.

We report in this work on the dependence of the scattering cross section on the exciting laser frequency for the two first-order peaks [allowed TO(Γ) and forbidden LO(Γ)], and the most prominent second-order bands [2TA($\Delta \rightarrow K$), 2TO(Δ, Σ, Λ), and 2LO(Γ)]. We follow, in particular, the resonances of the 1LO(Γ) and 2LO(Γ), which are the more dispersive over a wide range of temperature (10–300 K) to investigate carefully the difference between the energies of the "Raman" and optical gaps.[4,5] Section II deals with experimental details. The results are presented and discussed in Sec. III.

II. EXPERIMENT

The experiments reported here were performed in the near backscattering configuration on an x-ray oriented (110) face of an undoped single crystal ($n<10^{16}$ cm^{-3}) which was mechanically polished and polished-etched with Syton. The scattered light was analyzed with a Coderg T800 triple spectrometer coupled with a photon-counting system. The different lines of an Ar$^+$-ion laser were used to cover the spectral range of the E_1 gap. Second-order features were recorded at low speed (1 cm^{-1}/min) and several times to ensure the reproducibility of the measurements. We performed the low-temperature runs with a CF204 Oxford Instruments Cryostat.

The selection rules for first-order scattering (Γ_{15} symmetry for TO allowed and Γ_1-like symmetry for LO forbidden) have been checked within 5%.

To obtain the dispersion of the Raman cross section $\mathcal{R}$, the scattered intensity I must be corrected for the ω^4 law, the optical properties of the sample, and the spectral response of the setup $f(\omega_S,\vec{e}_S)$. ω_S and $\vec{e}_S$ are the frequency and the polarization vector of the scattered light. The expression of $\mathcal{R}$ is[10]

$$\mathcal{R}\propto\frac{I(\alpha_i+\alpha_S)n_i n_S}{\omega_S^4(1-R_i)(1-R_S)f(\omega_S,\vec{e}_S)}. \quad (1)$$

I is the scattered intensity per unit of incoming light power; R, α, and n are the reflection coefficient, absorption coefficient, and the index of

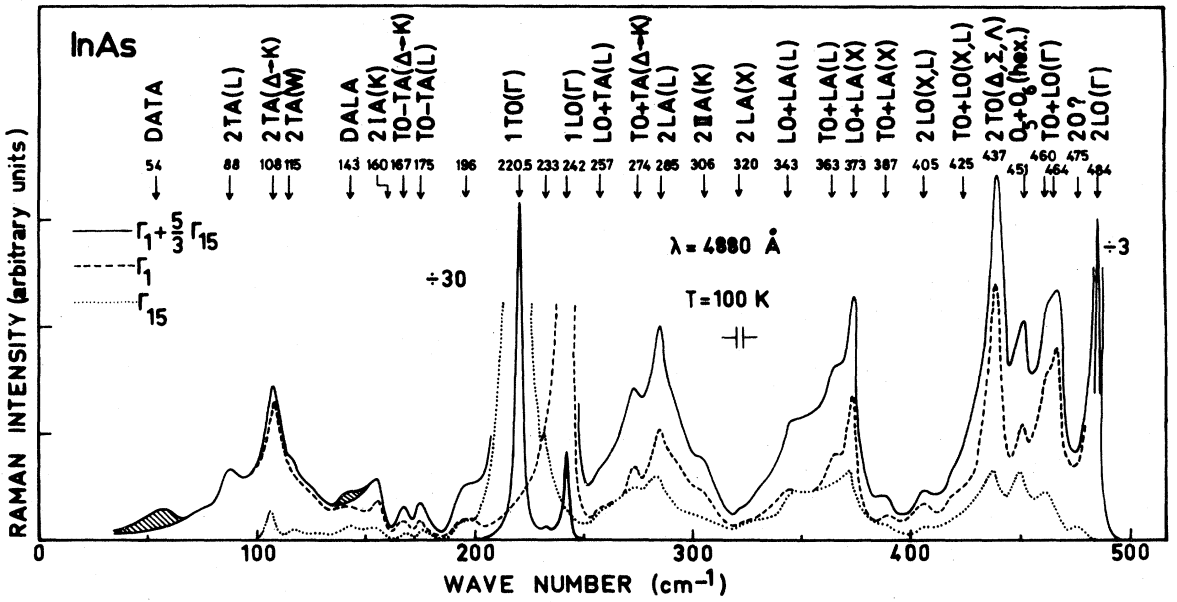

FIG. 1. Raman spectra of InAs obtained at 100 K with λ=4880 Å. Dashed line: Γ_1 component; dotted line: Γ_{15} component (from Ref. 9).

refraction of the crystal, respectively (i and S refer to incident or scattered light).

In the spectral range investigated (2.41–2.73 eV), the Raman tensor of CaF_2 is assumed to be not dispersive and we can write the corresponding scattered intensity as

$$I(CaF_2) \propto \omega_S^4 f(\omega_S, \vec{e}_S) . \quad (2)$$

If we neglect the small differences between the spectral positions of the bands we study in InAs and that of the peak of CaF_2 located at 322 cm^{-1} at 300 K, we can deduce from (1) and (2),

$$\mathcal{R} \propto \frac{I(\alpha_i + \alpha_S) n_i n_S}{I(CaF_2)(1-R_i)(1-R_S)} . \quad (3)$$

At 300 K the scattered intensity I was corrected using expression (3) with the reflectivity data of Philipp and Ehrenreich.[11] For other temperatures, due to the lack of a complete set of optical data, we correct I only for the ω^4 law and the spectral response of the setup through the normalization by $I(CaF_2)$. As a matter of fact, we checked at room temperature[12] that the corrections for the optical constants do not introduce any essential change in the shape of the E_1 resonance. The most important correction originates from the absorption coefficient. We choose not to make it to avoid additional errors that could be introduced by shifting the room-temperature absorption edge to higher energy.

III. RESULTS AND DISCUSSION

Table I summarizes the different structures that we studied. We give their frequencies at 100 K, their symmetries, and the corresponding selections rules. Figure 2 shows their resonances at 100 K around the energy of the E_1 gap. Resonances at 300 K have been published elsewhere.[12] We note in Fig. 2 and in subsequent figures, that the intensity of the scattered light is measured by the height of the structure. Dashed lines in Fig. 2 are guides for the eyes.

We investigate only the Γ_1 component of the second-order bands. As shown in Fig. 1 the 2TA($\Delta \rightarrow K$) and the 2LO(Γ) correspond mainly to that symmetry. Also the intensity of the Γ_{15} component of the 2TO(Δ, Σ, Λ) band was too weak to study its resonance significantly.

Figure 2 emphasizes the following points: (i) The

TABLE I. Frequency, symmetry, and selection rule characteristics of the different structures investigated.

Structure	Frequency (cm^{-1}) at 100 K[a]	Symmetry	Selection rule
1TO(Γ)	220.5	Γ_{15}	allowed
1LO(Γ)	242	Γ_1-like	forbidden
2TA($\Delta \rightarrow K$)	108	Γ_1	allowed
2TO(Δ, Σ, Λ)	437	Γ_1	allowed
2LO(Γ)	484	Γ_1-like	

[a] From Ref. 9.

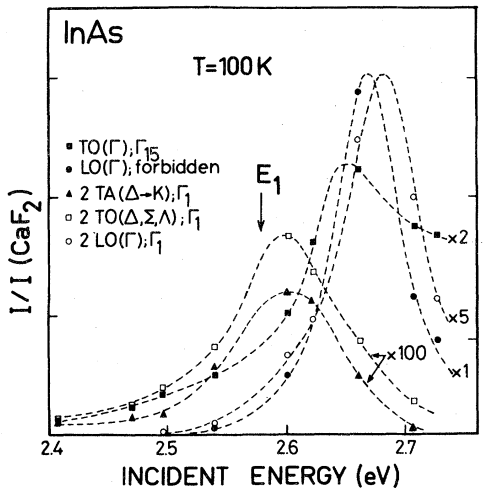

FIG. 2. E_1 resonance at 100 K of the structures quoted in Table I. Dashed lines are guides for the eyes. Values of the energy of the E_1 gap are from Ref. 29.

resonance of the forbidden first-order LO phonon is sharper than that of the allowed TO one. This is also true at 300 K (Ref. 12); (ii) this holds also for the second-order scattering. The 2LO(Γ), which corresponds to a frequency where the overtone density of states falls to zero and should be forbidden, shows a much sharper resonance than the allowed processes (2TA, 2TO); (iii) the shape of the resonances for the 1LO(Γ) and 2LO(Γ) scattering are similar. Their strengths from 300 to 100 K decrease much less than that of allowed processes.

From the data of Fig. 2 and those of Ref. 12, one deduces that the variations of the ratios $I(2TA)/I(2TO)$ and $I(2LO)/I(1LO)$ are well accounted for by the Bose-Einstein factor when the temperature varies from 300 to 100 K. On the other hand, this is not true for the ratio $I(2TO)/I(1TO)$. As we shall see in the former case the mechanisms which explain the corresponding scattering 2TA-2TO and 2LO-1LO are similar; they are different in the latter one (2TO-1TO). We shall discuss successively the resonances of the different structures in InAs according to the type of mechanism they are explained by.

A. Deformation-potential coupling

It has been shown[13] that for first-order allowed scattering the electron-phonon interaction is governed by the deformation-potential-type coupling. The shape of the resonance around the E_1, $E_1+\Delta_1$ gaps is well described by considering both inter- and intraband processes characterized by two independent deformation potentials.[14] The expression of the d_1 component[15] of the Raman tensor has been worked out in detail by Renucci *et al.*[16] and has the following expression:

$$d_1=\left(\frac{2\sqrt{2}}{\sqrt{3}}\frac{\chi^+-\chi^-}{\Delta_1}d^5_{3,0}-\frac{1}{2\sqrt{3}}\frac{d\chi}{d\omega_1}d^5_{1,0}\right)\frac{\langle\xi^2\rangle^{1/2}}{a}\,. \tag{4}$$

χ^+ and χ^- are the contributions to the electronic susceptibility χ of E_1 and $E_1+\Delta_1$, respectively, $d\chi/d\omega_1$ is the derivative of χ versus the energy of the E_1 gap, a is the cubic lattice constant, and ξ the amplitude of the displacement of an ion relative to its equilibrium position. The notation for the deformation potentials is the one used by Kane.[17]

The shape of the allowed TO(Γ) resonance shown in Fig. 2 is broad and asymmetric. It is essentially the same as the one obtained by Rubloff *et al.*[5] It has been successfully interpreted by Anastassakis *et al.*[6] using an expression similar to (4) but adding also a constant C to include the contribution to χ of terms nondispersive near E_1. $d^5_{3,0}$, $d^5_{1,0}$, and C were used as parameters to obtain an optimum fit to the experimental data. The ratio $d^5_{1,0}/d^5_{3,0}$ was found equal to -0.5 ± 0.3.[6]

$d^5_{3,0}$ refers only to the valence band while $d^5_{1,0}=d^5_{1,0}(\text{cond.})-d^5_{1,0}(\text{val.})$ has two components $d^5_{1,0}(\text{cond.})$ and $d^5_{1,0}(\text{val.})$ due to the contributions of the conduction and valence bands.[17] We can estimate $d^5_{3,0}$ and $d^5_{1,0}$ along the Λ direction in InAs using the values calculated by Zeyher[18,19] in InSb and GaAs. Indeed, to obtain by the $\vec{k}\cdot\vec{p}$ method the band structure of InSb and GaAs, the $\vec{k}=0$ energy levels and momentum matrix elements of the isolectronic α-Sn and Ge were successfully used.[20] On the other hand, for InAs (Ref. 20) the average values of the α-Sn and Ge parameters give good results. We thus estimate $d^5_{3,0}$ and $d^5_{1,0}$ in InAs along Λ taking the average value between GaAs and InSb. The values deduced in this way agree with those calculated by the $\vec{k}\cdot\vec{p}$ pseudopotential method.[21] As the valence and conduction bands in InAs are almost parallel along the Λ direction, except near Γ, we estimate $d^5_{3,0}$ and $d^5_{1,0}$ at a distance equal to $\frac{2}{3}$ of the Γ-Λ region away from Γ. We obtain[21] $d^5_{3,0}=37$ eV and $d^5_{1,0}=-12$ eV. The corresponding ratio $d^5_{1,0}/d^5_{3,0}=-0.3$ agrees, within the experimental error, with the value given by Anastassakis *et al.*[6]

For most of the two-phonon spectra in diamond- and zinc-blende-type semiconductors, the electron–two-phonon coupling was also found to be of the deformation-potential type[22] with the exception of the 2TO scattering in Ge (Ref. 16) and Si (Ref. 23) and the 2LO(Γ) scattering in polar crystals.[24,25] The former[16] is attributed to an iterative process involving the first-order-electron–one-phonon

deformation-potential interaction taken to second order; the latter is explained by an iterative electron–one-phonon Fröhlich-type interaction.[25]

When the two-phonon scattering is governed by a deformation-type coupling, the Γ_1 component of the Raman tensor is given by[16]

$$a_2 = \frac{4}{3}\frac{d\chi}{d\omega_1} D_1 \frac{\langle \xi_i^2 \rangle^{1/2} \langle \xi_j^2 \rangle^{1/2}}{a^2} . \quad (5)$$

i and j refer to the two phonons involved in the process and D_1 is the electron–two-phonon deformation potential of the Γ_1 component.

Figure 3 shows the resonances of the Γ_1 component of the $2TA(\Delta \rightarrow K)$ and $2TO(\Delta, \Sigma, \Lambda)$ structures at 300 K. As already mentioned these data are corrected using expression (3). They are fitted with expression (5) where we substitute $-d\chi/d\omega$ to $d\chi/d\omega_1$.[16] We use experimental values of χ.[11] The derivatives were replaced by finite differences because of the finite frequency of the phonon involved.[16] The solid and dashed-dotted lines in Fig. 3 represent such differences although they are labeled $d\chi/d\omega$. For a better fit these curves, deduced from optical measurements, had to be shifted to higher energies. These shifts differ according to the phonon which modulates the electronic susceptibility [~60 meV for the $2TA(\Delta \rightarrow K)$ and ~100 meV for the $2TO(\Delta, \Sigma, \Lambda)$]. This was found to be quite general[16, 23-25] and we shall discuss this point in length later on.

The agreement between experimental points and theoretical curves in Fig. 3 indicates that the scattering processes are controlled by a deformation-type mechanism involving only two band terms.

Using Eqs. (4) and (5) to fit the experimental data it is possible to determine the deformation potential D_1 for the $2TA(\Delta \rightarrow K)$ and $2TO(\Delta, \Sigma, \Lambda)$ scattering by comparison with the first-order scattering, provided $d^5_{1,0}$ and $d^5_{3,0}$ are known.[16, 26] With the values $d^5_{1,0}/d^5_{3,0} = -0.5$ (Ref. 6) and $d^5_{3,0} = 37$ eV (Ref. 21), we can determine D_1. It has been calculated for three different incident laser energies. The average values are

$$D_1[2TA(\Delta \rightarrow K)] = 350 \text{ eV},$$

$$D_1[2TO(\Delta, \Sigma, \Lambda)] = 2500 \text{ eV}.$$

Although these values should be regarded as significant within 50%, they follow, nevertheless, the trends already encountered for other IV and III-IV compounds.[16, 23-26]

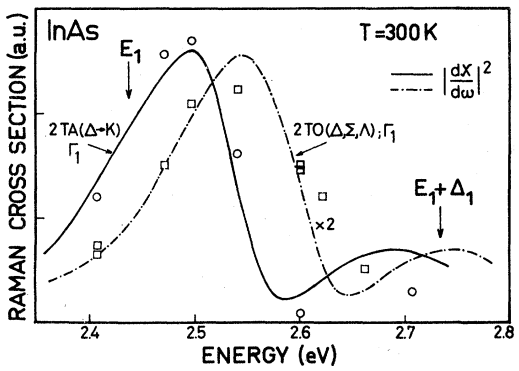

FIG. 3. E_1 resonance of the Γ_1 component of the $2TA(\Delta \rightarrow K)$ and $2TO(\Delta, \Sigma, \Lambda)$ at 300 K (from Ref. 12). The solid and dashed-dotted lines are theoretical curves (see text). Values of the energies of the E_1 and $E_1 + \Delta_1$ gaps are from Ref. 29.

B. Fröhlich coupling

Forbidden 1LO scattering has been discussed thoroughly by Martin and Falicov.[2] It corresponds to an intraband Fröhlich coupling and is proportional to the wave vector of the scattering phonon. For a two-dimensional critical point, Trommer and Cardona[25] have shown that the Raman tensor is proportional to the second derivative $d^2\chi/d\omega^2$ of the electronic susceptibility. As it is hazardous to derive experimental curves twice, these authors used a theoretical expression of χ. Near E_1, χ being well represented by a logarithm singularity, we have

$$\frac{d^2\chi}{d\omega^2} \propto [(\hbar\omega_1 - \hbar\omega) + i\eta]^{-1},$$

where $\hbar\omega_1$ is the energy of the E_1 gap and η is an energy broadening. To explain the strong dispersion of the $2LO(\Gamma)$ peak of Γ_1 symmetry near E_1, Trommer and Cardona[25] invoke an iterative electron–one-LO-phonon Fröhlich coupling.

Following the method explained in Ref. 25, we fit the experimental resonances of the $1LO(\Gamma)$ and $2LO(\Gamma)$ in InAs using the following expression:

$$I = \frac{I(\hbar\omega_1)}{\left[\left(\frac{\hbar\omega_1 - \hbar\omega}{\eta}\right)^2 + 1\right]^2}, \quad (6)$$

where $\hbar\omega_1$, η, and $I(\hbar\omega_1)$ (height of the resonance curve) are used as adjustable parameters. $\hbar\omega_1$ now defines the energy of the "Raman gap."

As displayed in Fig. 2, the resonances of the $1LO(\Gamma)$ and $2LO(\Gamma)$ scattering are sharper than the other ones. We thus decide to follow these resonances as a function of temperature to try to clarify the question of the energy of the Raman gap compared to that of the optical gap. Indeed for a number of compounds[16, 23-25] it has been found that, around the E_1 transition, the energy which corresponds to the maximum of the resonance (Raman gap) does not match the one measured by means of optical constants. Nevertheless in

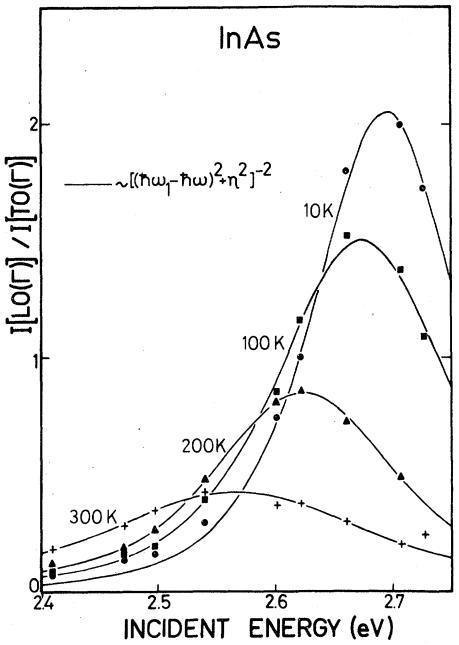

FIG. 4. E_1 resonance of the forbidden 1LO(Γ) as a function of temperature. Solid lines are theoretical curves (see text).

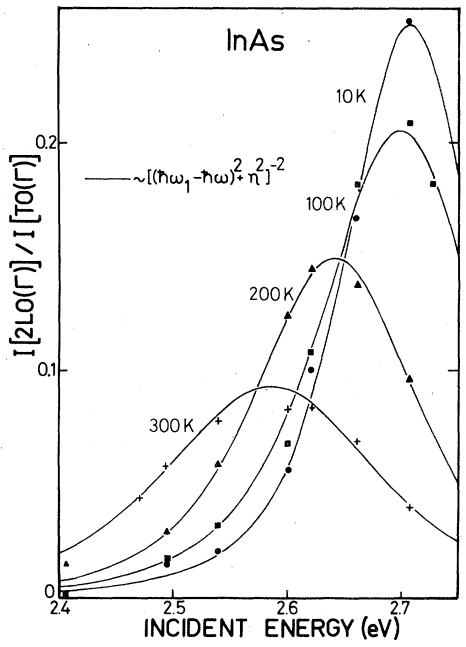

FIG. 5. E_1 resonance of the 2LO(Γ) as a function of temperature. Solid lines are theoretical curves (see text).

GaAs,[25] the situation was not so clear and the question was asked whether these shifts were of fundamental character.

Figures 4 and 5 display the resonances of the 1LO(Γ) and 2LO(Γ) over a large interval of temperature (10–300 K). The dependence of the scattered intensity upon frequency was measured relative to that of the first-order TO(Γ). The results are thus corrected for the incident laser power, the ω^4 law, the spectral response of the setup, and the optical properties of the sample as the difference in the frequencies of the 1TO(Γ) and 1LO(Γ) is negligible and that of the 1TO(Γ) and 2LO(Γ) not too large. Between 2.62 and 2.72 eV the TO(Γ) cross section is only slightly dispersive and the 1LO(Γ) and 2LO(Γ) resonances are thus well represented by the data of Figs. 4 and 5. These forbidden scatterings show a strong temperature dependence. It has been suggested that this is related to a strong excitonic contribution to the LO resonance.[4] The experimental data of Figs. 4 and 5 were reproduced with expression (6) using a least-squares-fit method. The agreement is excellent. This proves that the forbidden 1LO(Γ) and 2LO(Γ) scatterings are well accounted for by the intraband Fröhlich coupling. Another contribution could be induced by the surface electric field, but since we used an undoped crystal, it should be negligible.[25]

From the fits of Figs. 4 and 5, one deduces $I(\hbar\omega_1)$ to be the height of the resonance curve, $\hbar\omega_1$ the Raman gap, and η the broadening energy. These last two quantities are plotted in Fig. 6 as a function of temperature. We give, also, the

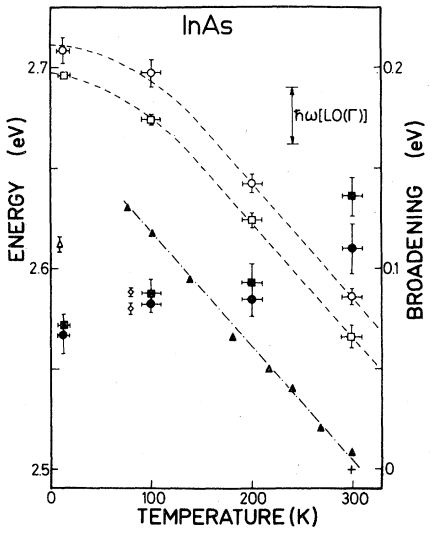

FIG. 6. Variations with temperature of the "Raman gap" and the broadening energy for the 1LO(Γ) and 2LO(Γ) resonances. Raman gap: □ 1LO(Γ), ○ 2LO(Γ), and broadening energy: ■ 1LO(Γ), ● 2LO(Γ). Corresponding error bars are indicated. Also plotted are values of the E_1 gap from different modulation techniques: △ Ref. 28, ▲ Ref. 27, ◇ Ref. 29, and + Ref. 30.

TABLE II. Experimental ratio of the strengths of the 1LO(Γ) and 2LO(Γ) resonances. Also given are the ratio of the Bose-Einstein factors relative to these two scatterings.

T (K)	10	100	200	300
$\frac{I(\hbar\omega_1)\eta[1\mathrm{LO}(\Gamma)]}{I(\hbar\omega_1)\eta[2\mathrm{LO}(\Gamma)]}$	1	0.91	0.71	0.56
$\frac{1}{\bar{n}+1}$	1	0.97	0.82	0.65

values of the E_1 optical gap obtained from several modulation techniques.[27-30]

The broadening parameter η is nearly equal for the 1LO(Γ) and 2LO(Γ) resonances and increases, as expected, with temperature. From Fig. 6 we can draw the following conclusions relative to the Raman gap:

(i) The energy of the Raman gap depends on the phonon involved [this was also true for the 2TA($\Delta \rightarrow K$) and 2TO(Δ, Σ, Λ), Fig. 3]. We note that the difference in energy between the maxima of the 1LO(Γ) and 2LO(Γ) resonances is not equal to the energy of the 1LO(Γ) phonon. This seems to exclude a resonance to the scattered photon.[31]

(ii) The energies of the Raman gaps are higher than those of the optical gaps around E_1 even if the latter are scattered. This holds also for the 2TA($\Delta \rightarrow K$) and the 2TO(Δ, Σ, Λ) (Fig. 3).

(iii) Between 100 and 300 K the energy of a Raman gap decreases linearly in a way similar to that of the optical one:

$$\left(\frac{d(\hbar\omega_1)}{dT}\right)_{\text{Raman}} = (-5.0 \pm 0.4) \times 10^{-4}\ \text{eV K}^{-1}$$

is to be compared with -5.5×10^{-4} eV K^{-1} obtained by thermoreflectance[27] and $(-5.0 \pm 0.4) \times 10^{-4}$ eV K^{-1} by wavelength modulation.[28]

(iv) Between 100 and 10 K a strong deviation from linearity appears. This was already seen in InSb where the 1LO resonance, measured by Yu and Shen[32] at 10 K and Keifer *et al.*[24] at 77 K, shows a maximum at the same photon energy. The phenomenon of saturation, at low temperature, occurs also for the energy of the optical gap.[28]

An estimate of the strength of the resonance is given by the product $I(\hbar\omega_1)\eta$. From Figs. 4 and 5 one can deduce this quantity for the 1LO(Γ) and 2LO(Γ) resonances as a function of temperature. Table II shows the corresponding ratio together with its value calculated by taking into account only the ratio of the Bose-Einstein factors. The agreement is very good, confirming the explanation of the 2LO(Γ) scattering in terms of an iterative 1LO(Γ) process.

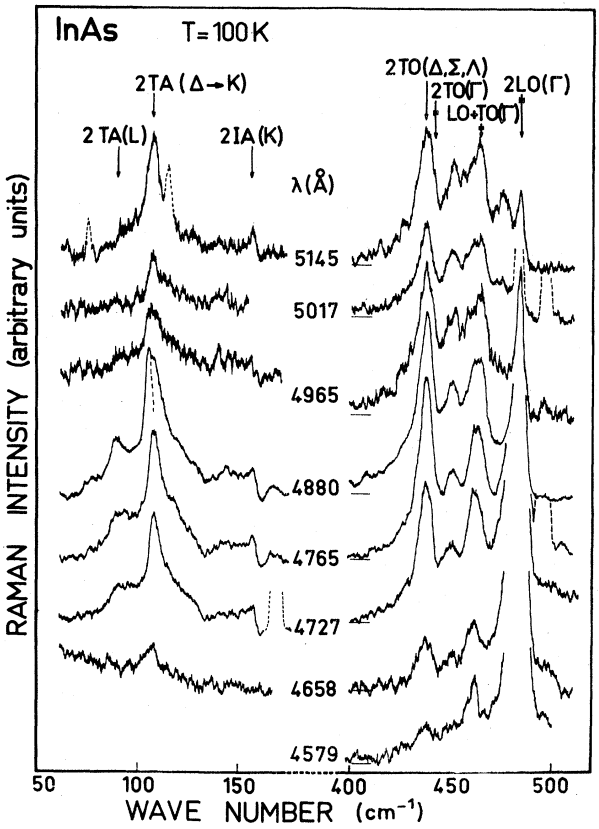

FIG. 7. Unpolarized second-order Raman spectra of InAs recorded at 100 K with several laser wavelengths.

Figure 7 displays unpolarized second-order Raman spectra of InAs recorded at 100 K for different laser wavelengths. Although the intensity of the 2TA(L) is weak, one sees that its resonance behavior is similar to that of the 2TA($\Delta \rightarrow K$). Also the TO+LO(Γ) follows the behavior of the 2LO(Γ), indicating that the Fröhlich coupling dominates. No resonance was observed for the 2TA(L) around the indirect $\Gamma_8^V - L_6^C$ gap.[33]

The study of the resonance in InAs over a wide range of temperature demonstrates unambiguously that the energy of a Raman gap differs from that of the optical one, but their variations with temperature are similar. The shift between them depends on the phonon involved but this shift is temperature independent. Although these results are deduced from the study of the sharp LO resonance, we believe they are general. There exists, currently, no theory to account for the dependence of the Raman gap upon the modulating phonon or to explain its temperature dependence.

[1]See, for example, M. Sinyokov, R. Trommer, and M. Cardona, Phys. Status Solidi B 86, 563 (1978).
[2]A. Pinczuk, E. Burstein, R. M. Martin, and L. M. Falicov, in *Light Scattering in Solids*, edited by M. Cardona (Springer, Berlin, 1975).
[3]W. D. Johnston, Jr. and I. P. Kaminow, Phys. Rev. 188, 1209 (1969).
[4]J. B. Renucci, M. A. Renucci, and M. Cardona, Solid State Commun. 9, 1235 (1971); Phys. Status Solidi B 49, 625 (1972).
[5]G. W. Rubloff, E. Anastassakis, and F. H. Pollak, Solid State Commun. 13, 1755 (1973).
[6]E. Anastassakis, F. H. Pollak, and G. W. Rubloff, Phys. Rev. B 9, 551 (1974).
[7]S. Buchner, E. Burstein, and A. Pinczuk, in *Light Scattering in Solids*, edited by M. Balkanski, R. C. C. Leite, and S. S. Porto (Flammarion, Paris, 1976), p. 76.
[8]S. Buchner, L. Y. Ching, and E. Burstein, Phys. Rev. B 14, 4459 (1976).
[9]R. Carles, N. Saint-Cricq, J. B. Renucci, M. A. Renucci, and A. Zwick, Phys. Rev. B 22, 4804 (1980).
[10]R. Loudon, J. Phys. 26, 677 (1965).
[11]H. R. Philipp and H. Ehrenreich, in *Semiconductors and Semimetals*, edited by R. K. Willardson and A. C. Beer (Academic, New York, 1967), Vol. 3, p. 535.
[12]R. Carles, N. Saint-Cricq, M. A. Renucci, and J. B. Renucci, in *Lattice Dynamics*, edited by M. Balkanski (Flammarion, Paris, 1978), p. 195.
[13]A. Pinczuk and E. Burstein, in *Proceedings of the 10th International Conference on the Physics of Semiconductors* (U. S. Atomic Energy Commission, Washington, D.C., 1970), p. 727.
[14]F. Cerdeira, W. Dreybrodt, and M. Cardona, Solid State Commun. 10, 591 (1972).
[15]R. Loudon, Adv. Phys. 13, 423 (1964).
[16]M. A. Renucci, J. B. Renucci, R. Zeher, and M. Cardona, Phys. Rev. B 10, 4309 (1974); and M. A. Renucci, Ann. Phys. (Paris) 9, 175 (1975).
[17]E. O. Kane, Phys. Rev. 178, 1368 (1969).
[18]M. Iliev, M. Sinyukov, and M. Cardona, Phys. Rev. B 16, 5350 (1977).
[19]R. Trommer, Ph.D. thesis, Stuttgart University, 1977 (unpublished).
[20]C. W. Higginbotham, Ph.D. thesis, Brown University, 1970 (unpublished).
[21]N. Saint-Cricq, M. A. Renucci, R. Carles, and J. B. Renucci (unpublished).
[22]M. Cardona, in Ref. 2, p. 1.
[23]J. B. Renucci, R. N. Tyte, and M. Cardona, Phys. Rev. B 11, 3885 (1975).
[24]W. Kiefer, W. Richter, and M. Cardona, Phys. Rev. B 12, 2346 (1975).
[25]R. Trommer and M. Cardona, Phys. Rev. B 17, 1865 (1978).
[26]B. A. Weinstein and M. Cardona, Phys. Rev. B 8, 2795 (1973).
[27]S. Antoci, E. Reguzzoni, and G. Samoggia, Phys. Rev. Lett. 24, 1304 (1970).
[28]R. R. L. Zucca and Y. R. Shen, Phys. Rev. B 1, 2668 (1970).
[29]M. Welkowsky and R. Braunstein, Phys. Rev. B 5, 497 (1972).
[30]M. Cardona, K. L. Shaklee, and F. H. Pollak, Phys. Rev. 154, 696 (1967).
[31]J. Shah, A. E. DiGiovanni, T. C. Damen, and B. I. Miller, Phys. Rev. B 7, 3481 (1973).
[32]P. Y. Yu and Y. R. Shen, Solid State Commun. 15, 161 (1974).
[33]P. B. Klein, H. Masui, Jun-Joo Song, and R. K. Chang, Solid State Commun. 14, 1163 (1974).